Chapter 2

Experimental Section

Chapter 2 provides a thorough explanation of the methods used to synthesize the materials and the many measurements required to characterize them.

Material synthesis and optimization is an important part of experimental research. This part starts with the methodological demonstrations and steps used in the preparation of various compounds which have been used in our whole research works. In the current work, solid-state reactions were used to create both $BiFeO_3$ co-doped (Tb, Mn, La, Al) and $GaFeO_3$ (Y, Er) doped compositions. This is followed by a variety of experimental techniques that are used to estimate various properties of the desired materials.

2.1 Material Synthesis Techniques

2.1.1 Solid-State Reaction Method

The conventional solid-state reaction method for oxide polycrystalline solid sample synthesis is one of the most widely used techniques which uses a stoichiometric mixture of different starting powder materials as precursors. At room temperature, solids do not react with each other over normal time scales and thus, it is required to heat them to quite high temperatures, often to 800 to 950 °C so that the reactions may take place at an appreciable rate. The important aspect which mainly decides the solid-state reaction's workability and rate is the surface area of the solids, the structural properties of the reactants, the reaction conditions, their reactivity, and the thermodynamic free energy change related to the reaction.

Throughout our research work, highly pure oxide powder materials have been used. The powders were taken in proper stoichiometry and then it was intimately ground for 3-4 hours in an agate mortar. This thoroughly mixed powder was then subjected to an initial heat treatment at the desired temperature (750-850 °C). Once the temperature reaches room temperature, the powder was reground, and then it was put in a muffle furnace in the air at different desired temperatures (up to 900 °C) for one to two days followed by intermittent

grindings to get the pure phase formation. This was then ground finely and it was used to carry out the powder X- ray diffraction (XRD) experiment at 300 K, to check the phase purity. Finally, this powder was pressed into pellets using the hydraulic press under suitable pressure for final sintering at some higher temperatures depending on the systems (950-1280 °C). These sintered samples were undergone through different experiments to explore their properties, for example, structural, magnetic, spectroscopic, optical, electrical, etc. The detailed processes have been discussed in the working chapters. The generalized flow chart for the solid-state reaction techniques is shown below:

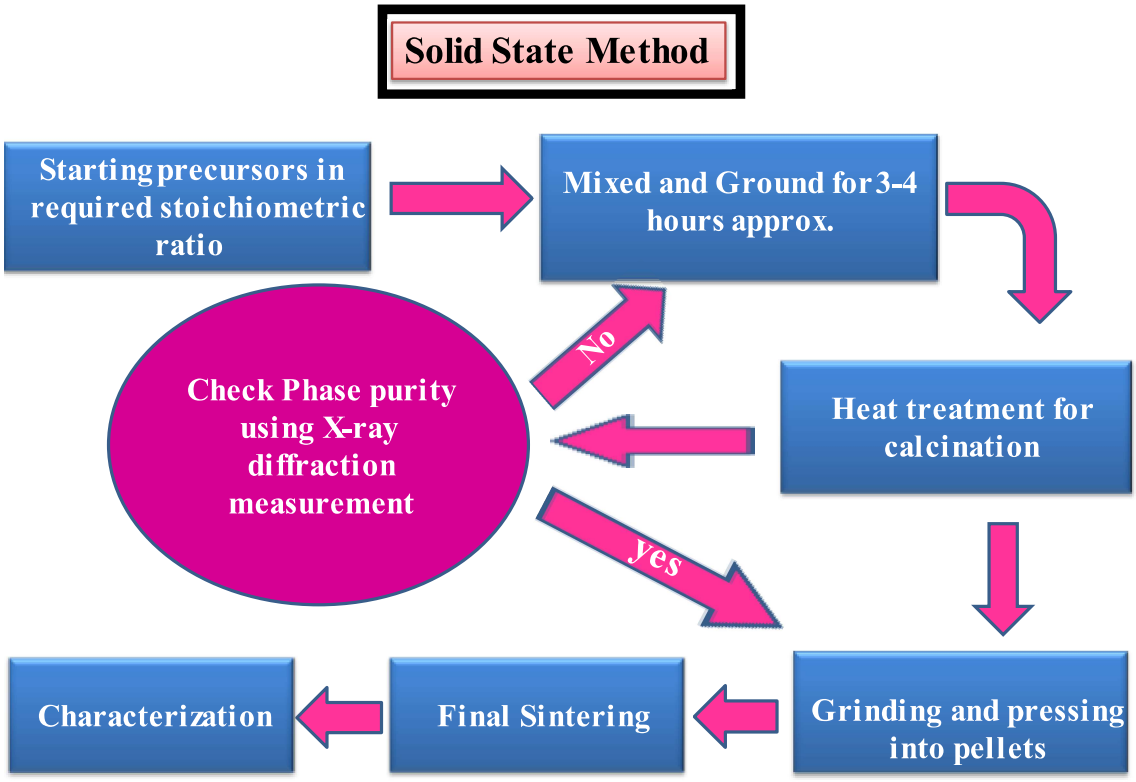

Figure 2.1: *The general flow chart for the solid-state reaction method.*

2.2 Experimental Characterization Tools

2.2.1 X-Ray Diffraction (XRD) Technique

When electromagnetic radiation interacts with a periodic structure, a diffraction

phenomenon occurs. X-rays are electromagnetic waves having a very short wavelength of the order of a few angstroms (1 Angstrom = 0.1 nm). The very short wavelength of X-ray denotes a high value of energy. When a monochromatic beam of X-ray is incident on the sample, the incident X-ray photons interact with the electrons of an atom in the sample. As a result, some of the photons are diffracted away from their original incident direction. Diffraction is the phenomenon in which the electromagnetic wave bend forms an obstacle if the obstacle's size is comparable to the wave wavelength. In crystalline materials, an inter-atomic distance lies in the range of 1 to 10 Å, which is the same order as X-ray wavelength. Constructive interference occurs only when the interference peaks are observed for a particular crystalline solid at particular angles. In the crystals, atoms are arranged periodically. Suppose the interference occurred by diffracted waves from the atomic planes satisfies Bragg's condition. In that case, it gives the X-ray diffraction pattern of a given material by measuring the intensity of diffracted waves with a variation of the X-ray incident angle. A lot of information can be obtained from the XRD pattern of the sample, i.e., information about the phase of the synthesized sample and provides the information of crystal structure and the dimension of the unit cell.

2.2.1.1 Bragg's Law

W. Lawrence Bragg and William H. Bragg have given the law for the diffraction of X-rays from the crystalline planes, known as Bragg's law [44]. Bragg's relation can elucidate the relation between the angle at which the beam diffracts from the crystalline structure and the wavelength used for X-rays. The relation can be expressed as:

$$2d\ sin\ \theta\ =\ n\lambda \tag{2.1}$$

Where n is an integer representing the order of diffraction, λ is the wavelength of the X-ray used, d is the interplanar distance of atoms and θ is the scattering angle or Bragg's angle. The intensity of diffracted X-ray is recorded as a function of the Bragg angle 2θ. The Rigaku-Miniflex II DESKTOP powder X-ray diffractometer, as shown in Figure 2.2, was

used to record the intensity *vs.* 2θ data. This diffractometer has a monochromatic X-ray source with Cu-K_α radiation (λ = 1.5418 Å) at 30 kV and 15 mA.

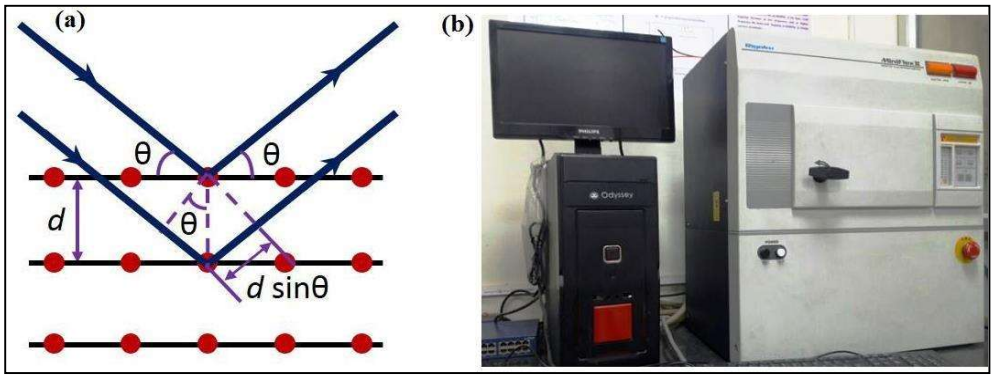

Figure 2.2: *(a) Photographic demonstration of Bragg's law (b) Actual photograph of Rigaku Mini Flex II DESKTOP X-ray diffractometer set up.*

2.2.2 Neutron Diffraction Technique

Neutron powder diffraction (NPD) is a powerful tool in the solid-state physics research field for determining the crystal structure as well as the magnetic micro-spin structure.

Neutrons are neutral and deeply penetrating unlike other radiation sources e.g., X-rays and electrons. The wavelength of the incident neutrons with a similar order of magnitude as the inter-atomic distances of crystalline solids enables one to study the aspects of condensed matter at the atomic level.

Eventually, all the diffraction experiments rely on Bragg's law and there are mainly two ways of experimenting. In the first process, a monochromatic neutron beam of wavelength λ_0 is targeted on a sample, and thus different inter-planar d-spacings are noted by moving a detector in a wide range of angles such that $\lambda_0=2d_{hkl}\sin\theta_{hkl}$, where the Miller indices (hkl) are related to the inter-planar spacing d_{hkl}. This method is usually used in most neutron diffraction facilities. However, there is an alternative method where the detector is kept fixed at an angle of θ_0 and the wavelength is varied. This can be done by utilizing a

white spectrum having a broad range of wavelengths and an energy-dispersive detector. In this case, the d - spacings are found using the following relation: $\lambda = 2dsin\theta_0$. The neutrons interact with matter in two main ways: firstly, the strong nuclear interaction which is related to the interaction occurring between the neutron and the nuclei of the sample, thus producing the nuclear scattering; secondly, the magnetic interaction, which is related to the interaction occurring between neutron spin and the atomic spins of the sample under investigation, thus giving rise to the magnetic scattering. Hence, the neutron diffraction technique has numerous advantages over the X-ray diffraction technique. First, the scattering length which characterizes the nuclear interaction is not dependent on the atomic number Z, unlike the X-ray scattering length which is proportional to Z. This is the reason why for X-rays, the atoms having lighter weight are almost invisible (especially in the case when other heavy atoms are present), on the contrary, for the neutrons, both the light and heavy atoms may have comparable scattering lengths. Secondly, as the neutrons have magnetic spin moments, it interacts with the atomic spins of the sample and is capable of giving precise information about the spin structure of a system. Hence, the neutron diffraction technique is ubiquitous in the field of magnetism research. All of our neutron diffraction measurements were performed on the PD2 (Powder Diffractometer-2) neutron powder diffractometer (λ =1.2443 Å) at the Dhruva reactor in Bhaba

Atomic Research Centre, Mumbai, India. The schematic diagram of the neutron diffractometer setup PD-2 is given below in Figure 2.3.

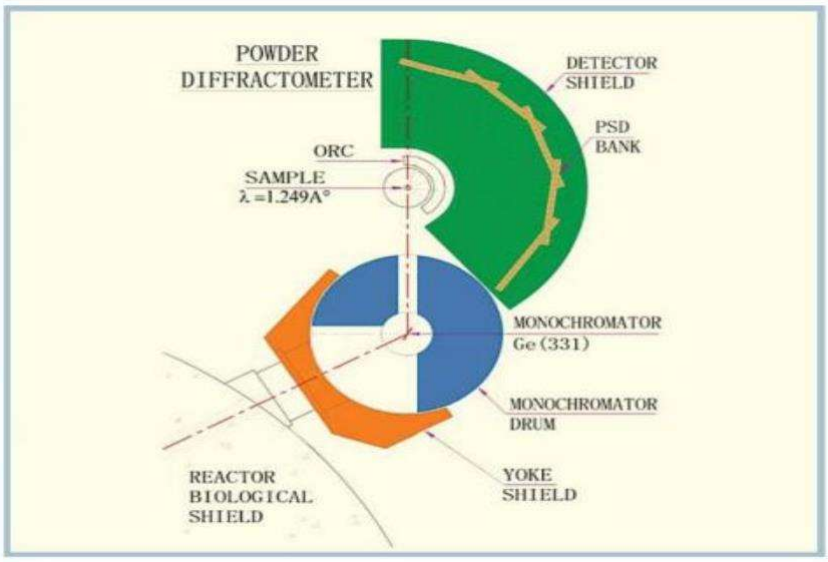

Figure 2.3: *Setup PD-2 (Powder Diffractometer-2) at Bhabha Atomic Research. Center, Mumbai, India.*

2.2.3 Magnetic Property Measurement System (MPMS)

Quantum Design (QD) MPMS is designed to examine the magnetic properties of small samples over a wide range of magnetic fields and temperatures. This device can measure a very small change in the magnetic field with enormous precision. It is controlled by several electronic controllers and provides data collection by a computer. Magnetic measurements are performed by extremely sensitive Superconducting Quantum Interference Device (SQUID). Thus, the MPMS is often called a SQUID magnetometer. The QD-MPMS is most widely used to measure the magnetic property through vibrating sample magnetometer (VSM) mode. A solenoid of superconducting wire (Superconducting magnet) is used in MPMS to produce a magnetic field up to ±7 Tesla (±70 kOe). The superconducting magnet and SQUID detector are both cooled by liquid helium. The sample chamber is cooled by the combination of both liquid nitrogen and liquid helium. MPMS covers the large temperature range measurement from 2 K - 380 K with a magnetization measurement sensitivity of 5×10^{-8} emu. In SQUID VSM, the sample vibrates sinusoidally

with the frequency ω about the center of the detection coils, where the signal picks as a function of the sample *Z(t)* position. Therefore, the expression for generated SQUID signal *V(t)* as a function of time t can be given as:

$$Z(t) = Sin(\omega t) \tag{2.2}$$

$$\text{and } V(t) = A\,Z^2(t) \tag{2.3}$$

$$V(t) = AB^2 sin^2(\omega t) \tag{2.4}$$

Here, *A* is a scaling factor relating to the magnetic moment of the sample and B is the sample vibration amplitude. In this system, the SQUID works as an extremely sensitive current-to-voltage converter and is inductively coupled with the detection coil. The SQUID functioning is based on Josephson tunneling effect and flux quantization in a superconducting ring. Due to the vibration of the magnetic sample through the coils, the coils generate the current in response to the disturbance in a local magnetic field. The SQUID feedback nulls the current in the pickup coils, so basically, there is no flow of current in them. Hence the SQUID voltage corresponds to the feedback current giving the value of sample magnetization. All the magnetic measurements of the present thesis are performed by QD-MPMS-SQUID-VSM, which is shown in Figure 2.4.

2.2.3.1 DC Magnetization and AC Susceptibility

To perform dc and ac magnetization measurements, mainly five major protocols are followed viz.

• Zero-field-cooled heating (ZFC): This protocol is followed when the sample is cooled from room temperature to the lowest temperature of measurement with zero magnetic fields. After switching on a required magnetic field, the data are recorded when the sample is heated to the desired T.

• Field-cooling (FC): FC condition is done by cooling the sample down to the lowest T of

measurement from room temperature in the presence of a magnetic field. M(T) data are recorded during the cooling cycle.

• Field-cooled heating (FCH): After obtaining FC condition, FCH protocol is followed by recording the data during heating in the presence of a magnetic field. MH measurement: MH-curves are hysteresis curves that are measured at constant T and here the magnetic field increases or decreases slowly which does not affect the dynamical magnetization processes.

• AC Susceptibility: Apart from the above-mentioned dc measurements, the real and the imaginary part of ac susceptibility (χ' and χ'' respectively) are also measured using the same instruments with varied T and f.

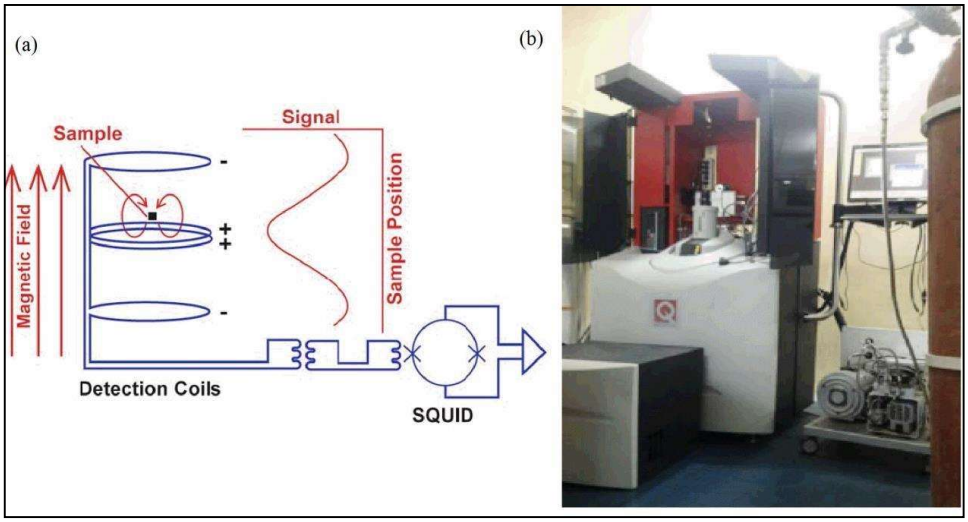

Figure 2.4: *(a) Schematic diagram of SQUID-VSM detection system. (b) Photograph of actual QD-MPMS measurement system.*

2.2.4 Dielectric Measurement

The dielectric measurement is a very important experimental method for the characterization of the semiconducting/insulating sample to prove different interesting phenomena like dipolar relaxation, dipolar ordering, ferroelectricity as well as electric conduction. In the dielectric study, we estimate the relative electrical permittivity (ε_r) i. e. dielectric constant of the materials. The relative electrical permittivity is a complex quantity

and thus expressed in real (ε_r') and imaginary parts (ε_r'') i.e., $\varepsilon_r = \varepsilon_r' + i\varepsilon_r''$ of the electrical permittivity. The ε_r' represents the total energy stored due to polarization in every cycle whereas ε_r'' represents the energy loss per cycle. These quantities may change depending on various parameters like temperature, pressure, frequency, electric and magnetic fields, etc. In our research study, we have estimated the dielectric constant from the capacitance measurement (as described in Chapter 3) using a Keysight E4980A Precision LCR meter, which is a famous impedance analyzer for dielectric spectroscopy with high precision and sensitivity. Here, the sample is put in the middle of two metallic electrodes, forming a parallel-plate capacitor-type arrangement. Then, the sample is biased with an alternating voltage signal *Vs*(*f*) and with an alternating current *Is*(*f*) using the LCR meter. At the same time, the impendence (*Z*) of the sample is calculated using Ohm's law, $Z = V(f)/I(f)$. This impedance is connected with the capacitance (C) of the sample as, $C = -i/2\pi fZ$ C, where I = √-1 (the imaginary factor) and *f* is the frequency of the alternating signals. A He-cooled closed cycle refrigerator (CCR) and Cryocon 32B temperature controller were used to control the temperature of the sample.

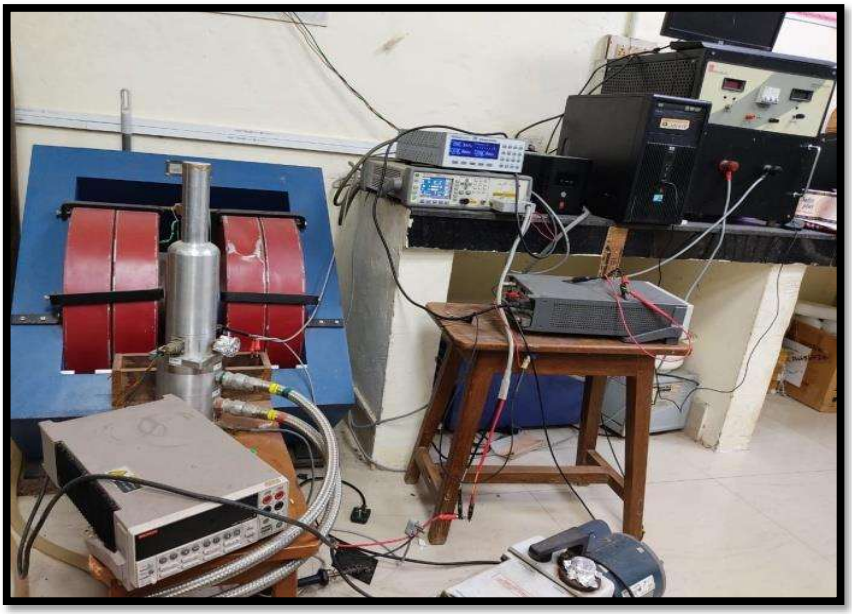

Figure 2.5: *Dielectric and magneto-dielectric measurement setup.*

The temperature of the sample was changed and controlled using a He-based CCR (closed cycle refrigerator) and a Cryocon 32B temperature controller. The sample used for this purpose was pelleted with a circular cross-section of ~5 mm radius and a few mm (1-2 mm) widths. Both circular faces of the pellets were coated with a silver paste which works as a metal electrode plate along with two thin copper wires attached at the same face. This prepared sample is then mounted in the CCR chamber and the electrometer was connected with the copper wires attached to the sample. The CCR chamber was put in a high vacuum using a rotary vane vacuum pump. And finally, the resistivity was measured at different temperatures. Moreover, the resistivity was also measured under the application of a magnetic field using an electromagnet up to 1.2 Tesla.

2.2.5 Raman Spectroscopy

"Raman spectroscopy" is based on the scattering of light through matter. Historically, after the discovery of Compton scattering in 1923, where X-ray is scattered by electrons and the wavelength of the X-ray is changed, C. V. Raman through the optical analog of the Compton effect and ultimately in 1928, Raman with his research partner Krishan was able to discover the Raman spectroscopy. When Raman did his first, he used sunlight as a source and his naked eye as a detector, due to the unavailability of advanced instrumentation. Afterward, the light was allowed to fall on a photographic plate. Later on, a lot of improvements have been made like the invention of a good excitation source with an advanced detector and a commercial Raman spectrometer was accessible. And this spectroscopy become an innovative technique to probe the qualitative and quantitative dynamic of atoms/ions/molecules in crystal using the scattering of light. While light scatters from the molecule/crystal, the most of photons get elastically scattered. The elastically scattered photons will possess the same energy as the incident photons. There is a very

small fraction of light (~1 photon out of 107 photons) which gets inelastically scattered with a change in their wavelengths by changing the rotational/vibrational/electronic energy of the molecule. This inelastic scattering is known as the famous Raman Effect (i.e., usually described as Raman shift) and the elastic scattering is recognized as Rayleigh scattering. The phenomena of the Raman effect can be explained based on the deformation of molecules in an electric field of strength E owing to the induced electric dipole moment, $P = \alpha E$ (α is the polarizability). The Raman shift can be observed only if the derivative of α is nonzero concerning Q (normal coordinates). When electromagnetic radiation interacts with the atom/molecule the electron clouds and bonds of the molecules get distorted. Due to this interaction, the atom/molecule gets excited to a virtual energy state from its ground state and thus becomes unstable. These excited molecules return to a different stable state (rotational or vibrational) by decreasing their energy by releasing a photon. The difference in energy between the initial stable state and the final stable of the molecule cause a shifting of the frequency of the emitted photon from the excitation energy. If the final state has large energy, then we get an emitted photon of a lower frequency than the excitation frequency and this shifting of energy of a scattered photon is known as stoke shift (Figure 2.6 (a)).

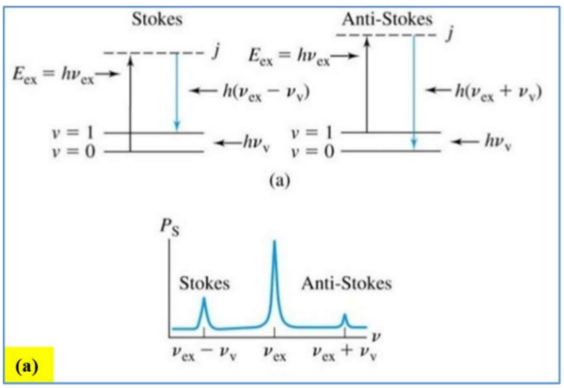

Figure 2.6: ***(a)*** *Illustration of Raman effect using energy level diagram* [64]*. (b) Display the picture of the Renishaw micro-Raman spectroscope used in our characterization.*

However, when the final state has lesser energy then we get an emitted photon with higher energy and this shifting is nominated as Anti Stokes shift. The Raman spectra are usually described in terms of wave numbers in the units of the inverse of length (cm^{-1}). In our study, we have used the Renishaw Raman spectrometer, which is shown in Figure 2.6 (b). Here, a monochromatic laser light of wavelength 532 nm, using a diode-pumped solid-state laser with a maximum power of 100 mW was used. To avoid heating the specimen, only 5% power was allowed to an incident on the sample. The laser beam was focused at a much shorter working distance over a 50 × long-distance objective connected with the Leica DM 2500M microscope. A dispersion grating with 2400 groves/mm with 50-micron slit width has been used to keep the constant phase throughout the experiments. The scattered light has been collected and passed to a detector. The data was collected using the supplied 4.0 software Spectrometer scanning and finally processing of data was finished.

We have used the temperature-dependent Raman spectroscopy technique (LabRam HR evolution spectrometer, maker: Horiba) to demonstrate the vibrational modes and how they modify depending on magnetic ordering or structural deformation. Here longitudinal and transverse vibrational Raman modes corresponding to a basic TI Sb_2Te_3 are shown using its atomic configurations.

2.2.6 UV-Vis (Ultraviolet-Visible) spectroscopy

The "ultraviolet-visible spectroscopy" is a typical absorption/reflectance spectroscopy in the ultraviolet-visible region of the electromagnetic spectrum. This spectroscopy has been extensively used to study the light-absorbing capacity of a material as well as to estimate the optical band gap of that material When the UV-Vis light of intensity *Io* passes through the sample and the intensity of transmitted light comes out to be *I* then the ratio *I/Io* is defined as the transmittance (*T*). In terms of percentage *T* expressed as,

$$\%T = \frac{I}{I_0} \times 100 \quad (2.5)$$

From the transmittance value, one can estimate the amount of light absorbed i. e. absorbance (*A*) in terms of transmittance (*T*) using the relation,

$$A = -\log\left(\frac{T}{100}\right) \quad (2.6)$$

This spectroscopy can also be used to examine the reflectance of any material. For this purpose, we measure the intensity of reflected light from that sample (*I*) using a UV-Vis spectrometer, and it is compared with the reflected light intensity (*IO*) of a reference material. Then the ratio *I*/*Io* is referred to as the reflectance of the sample. In the UV-Vis spectrophotometer, a diffraction grating is used which works as a monochromator and separates the dissimilar wavelengths of incident light by collecting the lights of several wavelengths. The usual radiation source used is usually a Tungsten filament (300 nm to 2500 nm), a deuterium arc lamp (190 nm to 400 nm), and nowadays people are using Xenon arc lamps and light-emitting diodes (LEDs) for visible lights. The detector used in this spectrometer is a charged couple device or a photodiode. In our study, we have the Lambda-35 UV–vis spectrophotometer from Perkin Elmer for the UV–visible absorption

measurement.

Figure 2.7: *UV-Visible spectrometer set up.*

2.2.7 X-Ray Photoemission Spectroscopy (XPS)

The XPS which is also called photoelectron spectroscopy for Chemical Analysis (ESCA), is a powerful technique used to collect chemical information about the surfaces of solid materials *viz*., oxidation states, elemental composition, ligand coordination, etc. Both the insulators and conductors can easily be investigated in surface areas from a few microns to a few millimeters in depth. The XPS is used as a surface-sensitive tool since it mainly identifies those electrons produced near the surface. The photoelectrons of interest have comparatively small kinetic energy. As a consequence of the inelastic collisions in the sample's atomic structure, photoelectrons producing more than 20 to 50 Å beneath the surface cannot escape with sufficient energy to be detected in this technique.

The sample under investigation is kept inside an ultrahigh vacuum ambiance (typically ~10-10 torr) and then it is exposed to a monochromatic, low-energy X-ray source. The X-rays incident on the sample results in the ejection of core-level electrons from sample atoms. The energy of a core electron produced in such a photoemission process is

a function of its binding energy and is a characteristic of the element from which it was emitted. As a matter of act, the primary data used for XPS is the energy analysis of the photo-emitted electrons. When the incident X-ray ejects the core electron, an outer electron fills the core hole. By the emission of an Auger electron or a characteristic X-ray, these energies get compensated. Further, in XPS Auger electron's energy can also be utilized along with the emitted photoelectrons. The following equation is used for the energy of each of the photoelectrons which is purposed by Ernest-Rutherford (1914):

$$E_{K.E.} = h\nu - (E_B + \phi) \qquad (2.7)$$

Here, E_B represents the binding energy of the electron, $h\nu$ represents the energy of the incident X-ray photons being used, $E_{K.E.}$ represents the kinetic energy of the electron that is measured by the spectrometer and the work function of the spectrometer is known as ϕ. This is illustrated in the schematic diagram Figure 2.8 (a). The different instrumental units of an XPS machine as demonstrated in the schematic Figure 2.8 (b),

1. Hemispherical electron energy analyzer
2. X-ray source
3. Ar-ion gun
4. Vacuum system
5. Neutralizer or electron flood gun
6. Multi-channel detector plates
7. Sample stage or holder
8. Electronic control units
9. Computer

X-ray photoemission spectroscopy (XPS) technique was used for our systems to understand the elemental valance states of the single crystals and how they modify for the as-prepared films. The Al-Kα X-ray source and the analytical aperture of diameter 400 μm

were used to measure the depth profile over the 2 mm × 4 mm area of the heterostructure by sputtering of 1 keV argon ions. The neutralizer attached to the XPS instrument was used for charge compensation, and the neutralized condition was uniform in both sputtering and measuring XPS spectra.

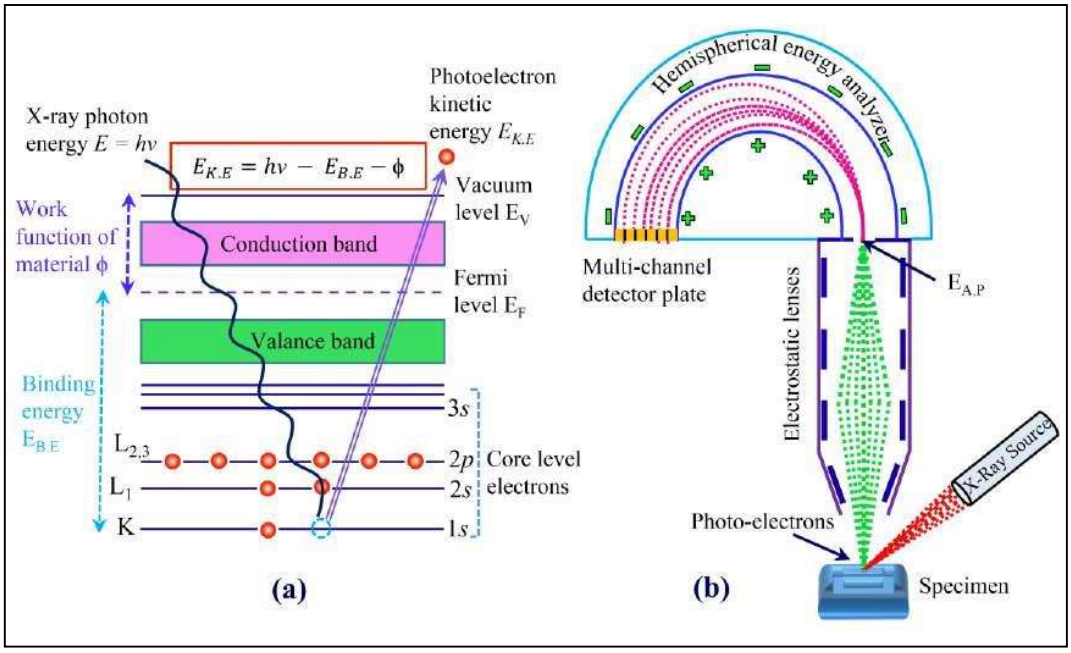

Figure 2.8: (a) Schematic diagram of a core-level-photoelectron emission process. (b) Hemispherical electron energy analyzer [65]